Turbulent Heat Transfer and Fluid Flow in an Unsymmetrically Heated Triangular Duct

C. A. C. Altemani
E. M. Sparrow
Fellow ASME

Department of Mechanical Engineering,
University of Minnesota,
Minneapolis, Minn. 55455

Experiments were performed to determine entrance-region and fully developed heat transfer characteristics for turbulent airflow in an unsymmetrically heated equilateral triangular duct; friction factors were also measured. Two of the walls were heated while the third was not directly heated. The resulting thermal boundary conditions consisted of uniform heating per unit axial length and circumferentially uniform temperature on the heated walls. Special techniques were employed to minimize extraneous heat losses, and numerical finite-difference solutions played an important role in both the design of the apparatus and in the data reduction. The thermal entrance lengths required to attain thermally developed conditions were found to increase markedly with the Reynolds number and were generally greater than those for conventional pipe flows—a behavior which can be attributed to the unsymmetric heating. The fully developed Nusselt numbers were compared with circular tube correlations from the literature, from which it was shown that the hydraulic diameter is not fully sufficient to rationalize the circular and noncircular duct results. However, excellent Nusselt number predictions were obtained by employing the Petukhov-Popov correlation in conjunction with the measured friction factors for the triangular duct. This approach may have general applicability for predicting noncircular duct heat transfer. The friction factor results also affirmed the inadequacies of the hydraulic diameter but supported a general noncircular duct correlation available in the literature.

Introduction

The use of noncircular ducts in heat exchange devices is motivated by a variety of potential benefits. For example, noncircular configurations have enabled the development of highly compact heat exchangers. A novel application of noncircular ducts is of current interest in connection with air-operated flat plate solar collectors. Inasmuch as airflow heat transfer coefficients are much lower than those of water flow, the circular tubes that are common in water-operated collectors have to be replaced with a duct configuration which affords greater heat transfer surface area. One such configuration is formed when the collector plate is a corrugated surface consisting of a succession of V grooves. When the corrugated plate rests on the underside insulation of the solar collector, an array of triangular ducts is created which constitute the passages for the airflow.

The research to be reported here is concerned with turbulent flow and heat transfer in a triangular duct. Although the initial motivation for the work was the aforementioned solar application, it was performed as a fundamental experimental study of convective heat transfer in a noncircular duct. Indeed, the experiments were carried out with a view to providing research results of impeccable quality which can serve as a standard against which analysis can be compared, as well as for direct input to design. The results were actually employed in this way in the latter portion of the paper. There, the well-known Petukhov-Popov circular-tube heat transfer correlation [1] was generalized to noncircular ducts by employing both the present heat transfer and friction factor data; the analytical-computational model of [2] for turbulent airflow in triangular ducts was also tested by comparison with the data.

The experiments were performed utilizing a sharp-cornered equilateral triangular duct, two walls of which were heated, while the third wall was not directly heated. The geometrical configuration and the heating arrangement were designed to yield a standard thermal boundary condition—uniform heat input per unit axial length and circumferentially uniform temperature on the heated walls. In the design of the apparatus, numerical finite-difference solutions were employed to aid in the selection of wall thicknesses, in the positioning of heating wire, and in the placement of thermocouples. Once the experimental data had been obtained, finite-difference solutions enabled evaluation of the heat leakage from the directly heated walls of the duct to the unheated wall; heat losses to the environment were also determined by finite differences.

Heat-transfer-related measurements were made which yielded both entrance region and fully developed heat transfer coefficients, as well as thermal entrance lengths. Pressure distributions were also measured, both for isothermal and nonisothermal conditions, from which friction factors were deduced. The experiments encompassed the Reynolds number range from 4000 to 60,000. In the low Reynolds number range, auxiliary data runs were made to explore the possible presence of natural convection effects. Air was the working fluid in all cases.

The relevant literature on turbulent heat transfer in triangular ducts will now be briefly reviewed. In an early investigation of equilateral ducts [3], average heat transfer coefficients for the duct as a whole were measured at high heating rates such that circumferential temperature variations of up to 55°C (100°F) were encountered. Later, in [4], measurements of heat transfer and friction characteristics were made in a narrow isosceles duct having an apex angle of 11.46 deg. Although the duct was 116 hydraulic diameters in length, thermally developed conditions were generally not attained. Somewhat more recently, experiments were performed in a rounded-corner equilateral triangular duct with a corner radius of curvature equal to 15 percent of the duct hydraulic diameter [5]. Intense heating rates were employed in those experiments, which resulted in a decrease of the Reynolds number from entrance to exit of as much as 50 percent. The foregoing citations encompass the available experimental literature on heat transfer.

The most complete study of turbulent fluid flow phenomena in equilateral triangular ducts is that of [2], which included both experiments and analytical-numercial predictions (based on the Buleev mixing length and turbulence kinetic energy model). The numerical solutions were extended to predict heat transfer coefficients, but without experimental confirmation.

Contributed by the Heat Transfer Division for publication in the JOURNAL OF HEAT TRANSFER. Manuscript received by the Heat Transfer Division March 21, 1980.

The Experiments

The experiments were performed in an open-loop airflow circuit which took air from a building-wide system and ultimately discharged it to the atmosphere. Along its path of flow, the air first encountered a succession of control and regulator valves and a filter, after which it was metered by one of two calibrated sharped-edged orifices which were respectively employed for high and low flow rates. It was then ducted to a plenum chamber fitted with baffles and a flow straightener—the plenum served as a transition from the circular tubing of the upstream piping system to the downstream triangular cross section.

The air exiting the plenum passed into an unheated equilateral triangular duct (made of plexiglass) which served as a hydrodynamic development section. The development section mated with the electrically heated test section. Both sections were of identical internal dimensions; side of triangle = 3.97 cm (1.56 in.), hydraulic diameter = 2.29 cm (0.902 in.). The respective axial lengths of the development and test sections were 53 and 106 hydraulic diameters. After passing through the test section, the air was thermally mixed in a specially designed mixing chamber, from which it was ducted to an outside exhaust.

The key components of the experimental apparatus will now be described. The description will highlight the novel measures that were employed to thermally isolate the heated test section in order to minimize possible extraneous heat losses or gains; another focus is the role of computer modeling as an adjunct to the apparatus design. Details of the apparatus and its design, beyond those given here, may be found in [6].

Heated Test Section. The triangular duct which served as the test section consisted of two relatively thick metallic walls and a thinner wall of a lesser conducting material. A cross-sectional view showing the duct wall configuration is presented in Fig. 1. The metallic walls were of aluminum, with a thickness of 0.952 cm (0.375 in.). The choice of aluminum of this thickness, taken together with the adopted heating method, was made with a view toward obtaining axially uniform heating and circumferentially uniform temperature on the two heated walls.

Heating was accomplished by means of electrical resistance wire embedded in longitudinal grooves machined in the outer face of each aluminum wall (see Fig. 1). Numerical finite-difference solutions of a model of this heating arrangement were employed to demonstrate that for the chosen wall material, wall thickness and heater-groove spacing, and for expected values of the heat transfer coefficient, uniform temperature is attained on the face of the wall that is in contact with the airflow. A generalized version of the analytical model is available in [7] along with representative results.

The third wall of the duct (i.e., the lower wall as pictured in Fig. 1) was made of plexiglass—chosen because of its moderately low thermal conductivity, light weight, surface smoothness, and availability in many sizes. The design objective for this wall was to approximate, as closely as possible, a zero heat flux surface. In practice, heat conduction across the surfaces of contact between the lower wall and the heated walls operates to oppose this objective. Both the size of the contact surface and thickness (0.318 cm, 0.125 in.) of the plexiglass wall were chosen as small as possible relative to mechanical constraints such as strength, wall flatness, and avoidance of leaks. To guide the trade-off between these mechanical constraints and the aforementioned heat transfer objective, the effects of both contact size and wall thickness on the heat flow via the plexiglass into the fluid were examined by means of finite-difference solutions detailed in Chapter 4 of [6]. The quantitative extent of this indirect heating of the fluid will be presented in the Results section of the paper.

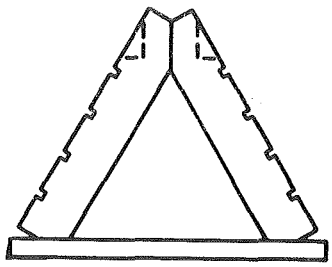

Fig. 1 Cross section of the heated test section

To facilitate the assembly of the duct, bevels were painstakingly cut into the edges of the aluminum walls as indicated in Fig. 1. The bevels extended along the entire 244-cm (8-ft.) length of the duct. The two aluminum walls were held together along their upper extremities by screws and nuts positioned at 10-cm (4-in.) intervals (the recesses for the screws and nuts are indicated by dashed lines in Fig. 1). Fastening of the aluminum side walls to the plexiglass bottom wall was accomplished by nylon screws positioned at the same interval—nylon being chosen to minimize heat conduction. To insure a leak-free seal, silicone rubber was packed into the V-shaped grooves at the intersections of the walls.

Thermocouples were installed at 14 axial stations along the test section. The use of the relatively thick-walled aluminum provided the options of surface mounting (on the rear face) or of embedding the thermocouples within the wall. The latter has the apparent advantage of placing the point of measurement closer to the inner surface of the wall, where the temperature value is desired, but also may cause a disturbance of the temperature field in the wall. Rear-face mounting also has both advantages and disadvantages. To resolve the issue, computational models were made for both situations (Chapter 4 of [6]), taking account of conduction in the wall, in the thermocouple leads, and in the insulation around the duct. These computations showed that wall embedding gives rise to a slightly more accurate temperature measurement and argued strongly for the use of iron-constantan wire rather than copper-constantan wire.

The thermocouples in the heated walls were positioned in drill holes which penetrated to within 0.19 cm (0.075 in.) of the inner surface. Prior to the insertion of the thermocouples, the holes were filled with a paste of copper-oxide cement, which subsequently hardened around the inserted thermocouples (copper-oxide cement is a moderately good heat conductor and an excellent electrical insulator). Three to five thermocouples were circumferentially distributed in the aluminum walls at each instrumented axial station. The coordinates of these stations will be evident from the data to be presented later.

At these same stations, a row of thermocouples was positioned along the spanwise centerline of the lower (plexiglass) wall. Owing to the thinness of this wall, external surface mounting of the thermocouples was the only viable option. Good thermal contact between the thermocouple junctions and the wall was ensured by the use of copper

Nomenclature

f = friction factor, equation (4)
h = local circumferential-average heat transfer coefficient
$\hat{h}$ = heat transfer coefficient for convection at lower wall
D_h = hydraulic diameter
k = thermal conductivity of air
k_p = thermal conductivity of plexiglass
$\dot{m}$ = mass flow rate
Nu = Nusselt number, hD_h/k
P = wetted perimeter of flow cross section
P_q = wetted perimeter of heated walls
Pr = Prandtl number
p = static pressure
Q' = local rate of heat transfer per unit length from heated walls to fluid
Q'_t = total rate of heat transfer per unit length from all walls to fluid
Re = Reynolds number
T = temperature
T_b = bulk temperature
$\hat{T}_b$ = bulk temperature for convection at lower wall
T_{bi} = bulk temperature at inlet
T_w = wall temperature
$\bar{u}$ = mean velocity
x = axial coordinate
x_{ent} = entrance length
μ = viscosity
ν = kinematic viscosity
ρ = density

oxide cement, whereas tape and epoxy were employed for strength and positive positioning.

For the determination of the axial pressure distribution along the duct, seven taps were installed in a row in one of the aluminum walls at a streamwise interval of ten hydraulic diameters. The tap in a given cross section was located at the circumferential midpoint of its host wall.

The instrumentation for the temperature and pressure readings will be described shortly.

Prior to the final assembly of the test section, the inner surface of the aluminum walls was hand polished to a high degree of smoothness. Special precautions were taken to eliminate burrs or other irregularities adjacent to the pressure tap holes.

Hydrodynamic Development Section; Mixing Box. As was noted earlier, the heated test section was preceded by a 53 diameters long unheated hydrodynamic development section. The development section was an equilateral triangular duct with inner dimensions identical to those of the test section. It was assembled from three pieces of plexiglass, two of which were bevelled in a manner identical to that for the aluminum walls of the test section. The assembly procedures were the same as for the test section, and the final assembled cross section is, with the exception of the heater wire grooves, well portrayed by Fig. 1.

The two side walls of the development section were 1.25 cm in thickness (½ in.), whereas the lower wall was 0.318-cm (0.125-in.) thick. It may be noted that the latter dimension is identical to the thickness of the plexiglass lower wall of the test section. In fact, to facilitate the assembly of the system, the test-section lower wall was designed to extend upstream, and thus to serve as the downstream end of the lower wall of the development section.

To monitor upstream thermal events, three thermocouples were installed in the wall of the development section (1, 10, and 20 diameters upstream of the test section). Two additional thermocouples, 10 and 20 diameters from the test section, were passed through the plexiglass wall into the airflow. These thermocouples, whose readings were always identical, yielded the inlet bulk temperature for the test section.

A mixing box was positioned at the downstream end of the test section for the determination of the exit bulk temperature. In view of the asymmetric heating of the airflow, the conventional three- or four-disk mixing box, with either centrally or peripherally positioned throughflow holes in the consecutive disks, is not sufficient for the mixing task. Instead, a special mixing box was designed to promote large scale transverse and circumferential motions (complete drawings are available in [6]). Thermocouple traverses immediately downstream of the mixing box indicated temperature uniformity to within 1 or 2 μV. For the actual temperature measurement of the mixed airflow, two thermocouples were employed, each installed in a six-legged star-shaped copper structure that spanned the cross section of the mixing box at its downstream end.

Minimization of Extraneous Heat Losses. The special measures employed to minimize extraneous heat losses will now be described. The need for extra care in the present experiments stems from the use of a thick-walled heated duct. Direct face-to-face contact of the upstream and downstream edges of the duct with the walls of the development section and of the mixing box would provide active conduction paths for heat loss and, therefore, the cross sections of those paths must be minimized. We will deal here with the adopted measures for curbing heat losses from the heated test section to the hydrodynamic development section, to the mixing box, and to the surroundings.

Consider first the mating between the aluminum walls of the test section and the corresponding plexiglass walls of the hydrodynamic development section. As shown in Fig. 2, full-face contact was avoided in favor of contact between a thin lamina A, which extends downstream from the plexiglass wall, and the aluminum wall. To prepare for this arrangement, a lap-like recess, 1.27-cm (0.5-in.) long and with a depth of approximately 0.046 cm (0.018 in.), was machined at the downstream end of the plexiglass wall. Then, a 2.54-cm (1-in.)-long phenolic lamina A was cemented into the recess, and the resulting

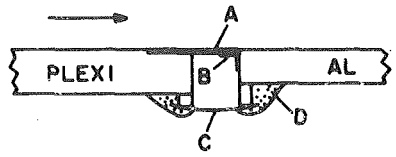

Fig. 2 Arrangement for minimizing heat conduction at the upstream end of the test section

surface was finished smooth. The forward edge of the phenolic extended 1.27 cm (0.5 in.) beyond the plexiglass, and it was this edge that contacted the aluminum.

To avoid leaks at the contact, a thin (0.005 cm, 0.002 in.) pressure-sensitive tape B was pressed in place as shown in Fig. 2. The main defense against leaks was made on the outer face of the walls. Here, a thicker plastic sheet C bridged between the two walls, with an airtight seal being achieved with silicone rubber D. To hold the just-described arrangement in place, a pair of narrow isolated plexiglass struts (not shown in the figure) bridged the gap just under the plastic sheet C.

Direct contact between the two aluminum walls and their upstream plexiglass counterparts was avoided by the aforementioned arrangement. With regard to the lower, not-directly-heated, wall of the test section (i.e., the plexiglass wall), it extends continuously upstream into the hydrodynamic development section. To minimize conduction along this wall, a spanwise cut was made from the outside surface which reduced the wall thickness to half the original value of 0.318 cm (0.125 in.). This cut was made at the cross section at which the heating was initiated.

Attention will now be turned to the measures used to minimize extraneous heat transfer between the downstream end of the test section and the mixing box. One of these measures was to reduce the conduction cross section of the aluminum walls by making a spanwise cut in each wall just upstream of the mixing box. The wall thickness at the location of the cut was 0.1 cm (0.040 in.) rather than the original thickness of 0.953 cm (0.375 in.). In addition, a spanwise cut was made in the lower (plexiglass) wall which locally reduced its thickness by a factor of two. Also, on the face of the mixing box which mated with the test section, numerous crater-like holes were drilled to reduce the cross section for heat conduction.

The measures for minimizing heat losses from the duct to the environment will now be discussed. To avoid heat conduction through structural supports, the entire assembly consisting of the hydrodynamic development section, the test section, and the mixing box was suspended by 0.043-cm (0.017-in.) dia nylon line at five axial stations. The nylon line was carefully monitored for stretch and sag, and none was encountered after an initial break-in period.

The aforementioned assembly was positioned within an insulated chamber of cross sectional dimensions 25 × 25 cm (10 in. × 10 in.). The chamber walls were of styrofoam, leaving a hollow cavity 10 × 15 cm (4 × 6 in.) for the apparatus. Silica aerogel powder insulation, which has a thermal conductivity less than that of air, was poured into the cavity around the apparatus.

The other parts of the piping system were lagged with fiberglass insulation.

Other Instrumentation. All thermocouples were made from 30-gage, calibrated iron and constantan wire. After installation of the thermocouples, they were led out of the insulation enclosure in a single bundle which terminated in a thermocouple junction box which contained connectors and switches. The box also contained aluminum bars and insulation to promote temperature uniformity. Thermocouple emfs were read with a Hewlett-Packard 3465A digital multimeter with a smallest digit of 1 μV.

For the test section pressure distribution, the pressure signals were sensed by a Baratron solid-state capacitance-type meter capable of being read to as low as 10^{-3} torr. The Baratron provided a digital output which was read by the aforementioned HP multimeter.

The test section power input was regulated to ensure constancy and was read by a specially calibrated electrodynamometer wattmeter with a full-scale accuracy of 0.25 percent.

Data Reduction

The main objective of the data reduction procedure was to yield axially local heat transfer coefficients for the heated walls of the triangular duct, both in the thermal entrance region and in the thermally developed region. The coefficients to be determined will represent circumferential average values at each axial station. Friction factors will also be deduced from the measured pressure distributions.

The local circumferential-average heat transfer coefficient for the heated walls is defined here as

$$h = (Q'/P_q)/(T_w - T_b) \tag{1}$$

where Q' is the rate of convective heat transfer per unit axial length from the heated walls to the fluid, and P_q is the wetted perimeter of the heated walls. The temperatures T_w and T_b respectively represent the values for the heated wall and the bulk. It is worthy of note that all of the wall-embedded thermocouples (i.e., in the aluminum walls) at any axial station gave temperature readings within 0.02°C of each other. Therefore, the heated walls may be regarded as being circumferentially uniform in temperature. All quantities in equation (1) pertain to a given axial station x.

In equation (1), only T_w is directly measured, whereas Q' and T_b are obtained from the data reduction procedure (P_q is equal to 7.92 cm (3.12 in.)). The starting point in the determination of Q' is the electric power dissipated in the resistance wire situated in the longitudinal grooves on the rear faces of the aluminum walls.[1] Two corrections were applied to the power dissipation per unit length in order to obtain Q'. One of these is for the heat loss from the duct outer surfaces to the environment via conduction through the insulation. The other is for the heat which flows by conduction from the heated walls into the plexiglass wall (i.e., the lower wall) and then passes into the airstream by convection at that wall. The latter heat flow is, in fact, not a heat loss; rather, it causes a rearrangement of the surface locations at which heat enters the airstream.

The determination of these two corrections involved a lengthy computation which is described in detail in [6] and will be discussed here only in broad terms. For the heat loss through the insulation, a two-dimensional, finite-difference conduction network was set up to accommodate the irregular solution domain encompassing the outer walls of the triangular duct and the somewhat irregular rectangular boundaries of the two zones of insulation (silica aerogel and styrofoam). The temperature inputs needed for these finite-difference solutions included the surface temperatures of the aluminum and plexiglass walls and the temperature of the air in the surroundings. Of these, the temperatures of the aluminum and of the surroundings were known from direct measurement, but the plexiglass surface temperature varies with spanwise position and only the mid-span value is available from measurement. The needed spanwise temperature distribution was obtained from the calculated temperature field in the plexiglass wall, the determination of which will now be described.

As already noted, heat is conducted into the plexiglass wall through its surfaces of contact with the heated aluminum walls and then flows by convection into the airstream. A fine-grid, two-dimensional finite-difference conduction network was superposed on the plexiglass wall to facilitate determination of the temperature distribution and the convection heat transfer. This computation was elevated from the routine by a philosophical issue related to the convective boundary condition.

To explore this issue, let y denote the direction normal to the inner surface of the plexiglass wall. Then, at that surface

$$-k_p(\partial T/\partial y) = \hat{h}(T - \hat{T}_b) \tag{2}$$

where k_p is the thermal conductivity of the plexiglass. The quantities $\hat{h}$ and $\hat{T}_b$ respectively represent the heat transfer coefficient and bulk temperature that are relevant to the convective heat transfer at the plexiglass surface. A careful study of the problem reveals that either $\hat{h}$ or $\hat{T}_b$ must be provided as input and, with that, the solution will yield the other of the two via an iterative procedure which makes use of the measured temperature at the mid-span point on the rear face of the wall. The solution also makes use of the measured temperature of the aluminum walls, which is assumed to prevail at the interface with the plexiglass wall.

Both options were explored. In one, $\hat{h}$ was taken equal to the average heat transfer coefficient at the heated walls of the duct, while $\hat{T}_b$ was treated as an unknown. In the other, $\hat{T}_b$ was set equal to the bulk temperature for the cross section as a whole and $\hat{h}$ was the unknown. There was little practical effect of using one option versus the other, as reflected in the fact that the extreme difference in the resulting heat transfer coefficients for the *heated walls* was only three percent.

For the authors, the first option is more satisfying on physical grounds and, therefore, it has been used for the final data-reduction computations. We do not believe that the bulk temperature T_b, which is primarily set by the heat transfer rates at the aluminum walls, has very much influence on the rate of convective heat transfer at the plexiglass wall;[2] in a real sense, T_b is quite remote from the plexiglass wall. Furthermore, considering the similarity of the flow pattern adjacent to all three walls, it is not unreasonable to use the same h at the plexiglass wall as at the other walls.

The numerical solutions for the plexiglass wall yield the rate at which heat passes out of the heated walls at the surfaces of contact with the plexiglass. This, in turn, completes the determination of Q' for equation (1). These computations were performed at each instrumented axial station. The foregoing description was intended to sketch the broad outlines of the computation procedure, but not to reproduce the details given in [6].

The bulk temperature appearing in equation (1) was computed by a step-by-step marching procedure that moved downstream along the duct, making use of the net heat transfer to the airstream at each station.

The effects of axial heat conduction in the aluminum walls were also examined. It was found that within the accuracy of the temperature instrumentation, significant effects of axial conduction could not be identified except at the most upstream stations at low Reynolds numbers. Owing to the uncertainty of the axial conduction corrections (i.e., large changes in $\partial^2 T/\partial x^2$ in response to small temperature uncertainties), the questionable data points will be omitted from the forthcoming presentation of results (see uncertainty analysis in Chapter 5 of [6]).

Once the local heat transfer coefficient had been determined from equation (1), the local Nusselt number was evaluated from

$$\mathrm{Nu} = hD_h/k \tag{3}$$

where D_h is the hydraulic diameter of the duct (2.29 cm, 0.902 in.) and k is the thermal conductivity of the airstream at the local bulk temperature.

The measured axial pressure distributions yielded, in each case, a straight line on a p versus x diagram, the slope of which was determined from a least-squares fit. This information was recast in dimensionless form via the friction factor

$$f = (-dp/dx)D_h/\tfrac{1}{2}\rho\bar{u}^2 \tag{4}$$

where $\rho\bar{u}^2$ was evaluated at the midpoint of the axial length over which p was measured.

The heat transfer and friction factor results are parameterized by the Reynolds number Re defined as

$$\mathrm{Re} = \bar{u}D_h/\nu = 4\dot{m}/\mu P \tag{5}$$

in which $\dot{m}$ is the mass flow rate and P is the perimeter of the walls which bound the flow cross section. For the actual evaluation of Re,

[1] The wattmeter reading was corrected to take account of ohmic dissipation in small segments of heating wire that lay outside the grooves. Also, thermocouple lead losses, which were ~0.1 percent, were prorated uniformly along the duct.

[2] The calculated convective heat transfer rate at the plexiglass wall ranged from three to ten percent of the total convective input to the air over the Reynolds number range from 59,000 to 4000 (see Table V, p. 136 of [6]).

the rightmost term of equation (5) was used, with μ at the local bulk temperature.

In general, property variations did not play a major role in the results. The maximum wall-to-bulk temperature difference was about 10°C (18°F), and the maximum bulk temperature rise from inlet to exit was of the same general magnitude.

Results and Discussion

The main focus of the presentation that follows will be the heat transfer results. Friction factors will also be presented, and they will be employed in correlating the fully developed heat transfer coefficients. To avoid interrupting the smooth flow of the heat transfer presentation, initial attention will be directed to the friction factor results.

Friction Factors. The friction factor results are plotted as a function of the Reynolds number in Fig. 3, where the open circles represent the isothermal data and the blackened circles correspond to the heat transfer runs. These two sets of data are nearly coincident and show the trend of f decreasing with Re that is typical of flow in smooth ducts.

Three literature correlations are shown in the figure in order to provide a comparison with the present results. The two uppermost curves respectively represent the Blasius and Prandtl circular tube correlations, which were applied here by employing the hydraulic diameter as the characteristic dimension. The comparison shows that the hydraulic diameter concept is not sufficient to rationalize the difference between the tube and triangular duct geometries, leaving an accuracy gap for f of 10 to 15 percent. The lower curve represents a general noncircular duct friction factor correlation [8] which was specialized to the present configuration. In the range of Re >7000, the present data agree with the correlation within two percent, on the average, thereby affirming its validity for the equilateral triangular duct. Since the correlation was developed for fully turbulent flow, the larger deviations at lower Reynolds numbers are not unexpected.

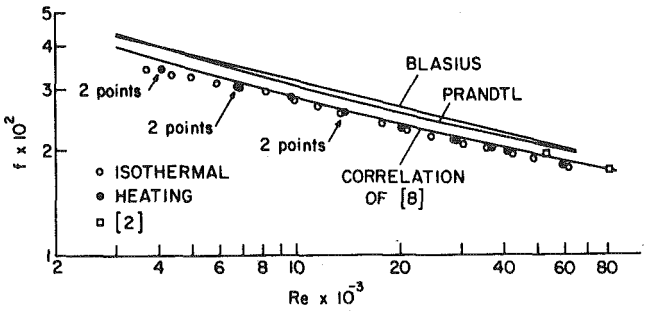

Fig. 3 Friction factor results

The square data symbols, which represent experimental results from [2], lie slightly above the present data. Finite difference solutions were also performed in [2] for the Reynolds number range between 40,000 and 300,000. For Reynolds numbers between 40,000 and 60,000, the predicted friction factors are about two percent lower than those given by the correlation of [8], which means almost exact agreement between the predictions and the present data. This agreement lends support to the computational model used in [2].

Temperature Distributions. Heat transfer data runs were made for eight Reynolds numbers between 4000 and 59,000. The measured axial temperature distributions display an interesting evolution in shape as a function of the Reynolds number, which is fully documented in [6]. Here, it will be sufficient to show results for two Reynolds numbers, one high and one low (59,130 and 6740), in order to illustrate the trends, and Figs. 4 and 5 have been prepared for this purpose.

In these figures, the temperature is made dimensionless in the form

$$(T - T_{bi})/(Q'_t/k) \tag{6}$$

In this expression, T_{bi} is the inlet bulk temperature and k is the thermal conductivity of the air at the mean bulk temperature. The quantity Q'_t is the total rate of heat transfer to the air per unit axial length, encompassing contributions from the directly heated walls and from the indirectly heated lower wall. Since T_{bi}, Q'_t, and k are fixed constants for each data run, the axial variation of the dimensionless group of equation (6) is a true reflection of the axial temperature variation.

In each figure, there are three sets of data points. The uppermost set depicts the temperature variation along the heated walls (as noted earlier, the temperature of the heated walls is circumferentially uniform). The other two sets, both of which are in the lower part of the figure, respectively depict the calculated values of the bulk temperature and the measured temperatures along the midspan of the rear face of the lower wall.

Attention may first be turned to the high Reynolds number results, Fig. 5. The temperature distribution on the heated wall displays a classical pattern that reflects the uniform heating condition—namely, an initial rapid rise that evolves into an ascending straight line which parallels the temperature rise of the bulk. The bulk temperature itself departs only very slightly from a straight line, the departures being due to slight variations in the heat losses along the duct. The region in which there is parallelism between the heated-wall and bulk temperatures grows larger as the Reynolds number decreases.

Figure 5 also shows that the midspan temperatures on the lower wall fall below the bulk temperature at the higher Reynolds numbers, and this relationship continues to prevail for all Re > 10,000. There

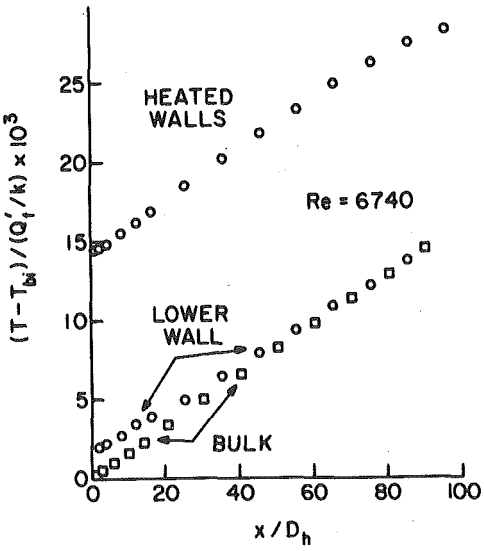

Fig. 4 Axial temperature distributions, Re = 6740

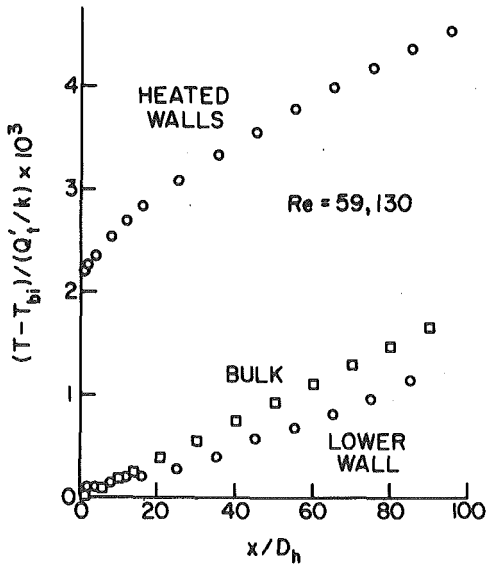

Fig. 5 Axial temperature distributions, Re = 59,130

is a tendency for the two distributions to become parallel at the most downstream stations. That the temperature of the lower wall is relatively low at these Reynolds numbers is indicative of the low rate at which heat is conducted into the lower wall from the directly heated walls. This low rate of conduction is the result of the relatively efficient convective heat transfer from the directly heated walls to the airstream, which makes the conduction leakage path to the plexiglass relatively unattractive.

The fact that the rear-face midspan temperature of the lower wall falls below the corresponding bulk temperature should not be taken as an indication that heat is being transferred from the airstream to the wall. In the lower part of the flow cross section, there is a zone of relatively low-temperature air (i.e., temperatures lower than the bulk temperature). It is the temperatures of the air in that zone, rather than the bulk temperature, which controls the magnitude and direction of the convective heat transfer at the lower wall.

The temperature distributions for Re = 6740 (Fig. 4) are quite different from those for Re = 59,130 which were just discussed. These differences evolve progressively with decreasing Reynolds number, as is evidenced in the successive figures presented in [6]. The main characteristics of the low Reynolds number distributions are: (1) parallelism between the heated-wall and bulk temperature distributions that is in force along most of the length of the duct, (2) temperatures on the lower wall that exceed the bulk temperature, and (3) a droop of the heated-wall temperature distribution near the downstream end of the duct.

The first of these characteristics implies a very short thermal development length, and we will return to this matter shortly when the Nusselt number results are presented. The second and third characteristics indicate the strengthened role of heat conduction which results from the less efficient convective heat transfer at the directly heated walls when the Reynolds number is low. Thus, the droop in the heated-wall temperatures at the downstream end of the duct is due to extraneous conduction to the mixing box. Furthermore, conduction from the heated walls into the lower wall is responsible for the elevation of the latter's temperature above the bulk.

Nusselt Numbers and Thermal Entrance Lengths. Circumferential-average Nusselt numbers for the heated walls have been determined at a succession of axial stations by employing the data reduction procedures described earlier. These results are presented in Fig. 6, where the Nusselt number is plotted against the dimensionless axial coordinate x/D_h ($x = 0$ corresponds to the beginning of the heated test section). The figure displays axial distributions for eight Reynolds numbers in the range from 4070 to 59,130. Supplementary data runs for the two lowest Reynolds numbers and for Re $\simeq$ 29,000 yielded results so close to those in the figure that they could not be plotted separately.

Examination of the figure shows the expected trend whereby higher Nusselt numbers correspond to higher Reynolds numbers. Also, the curves for the higher Reynolds numbers display the classic developmental pattern characterized by relatively high heat transfer coefficients near the inlet which decrease smoothly throughout the thermal entrance region and ultimately attain an axially unchanging fully developed value. It is, however, interesting to note that at these Reynolds numbers, the entrance length, as measured in terms of the hydraulic diameter, is rather long; in fact, fully developed conditions are just barely achieved. As the Reynolds number decreases, the length of the entrance region decreases markedly. (Note that at the two lowest Reynolds numbers, data affected by axial conduction have not been presented).

For a quantitative characterization, the thermal entrance length may be defined as the axial location at which the heat transfer coefficient approaches to within five percent of its fully developed value. Entrance lengths corresponding to this definition are presented in Fig. 7, where the marked increase with Reynolds number is clearly evident. To obtain perspective about these results, the relevant literature may be examined. For triangular-duct heat transfer, no entrance lengths were determined in [3] (only average coefficients were measured), while in [5] the large property-related Reynolds number variations along the duct make the definition of an entrance length

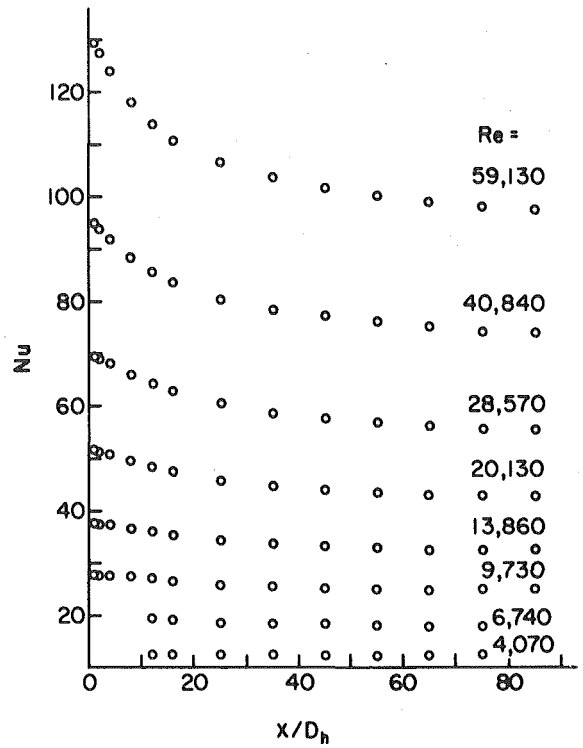

Fig. 6 Axial distributions of the Nusselt number

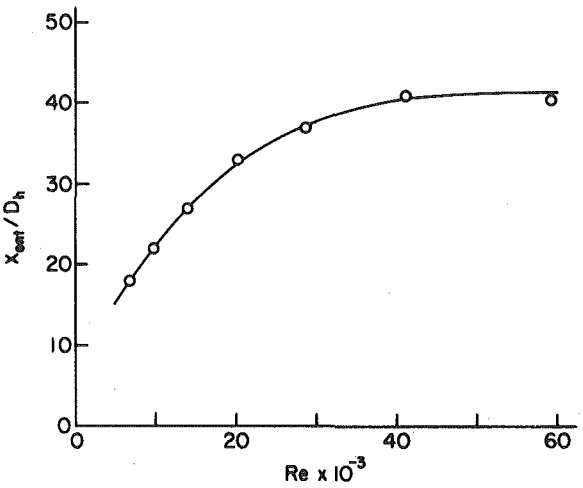

Fig. 7 Thermal entrance lengths based on a five percent approach of Nu to its fully developed value

quite uncertain. In [4], for a small apex-angle triangular duct, very large entrance lengths were encountered.

Also relevant are the experiments of [9] involving turbulent airflow in a circular tube heated on only half of its circumference. There, it was found that the thermal entrance lengths were considerably greater than those for a circumferentially uniformly heated tube; furthermore, the entrance lengths increased markedly with Reynolds number, as in the present experiments.

From the foregoing, it can be concluded that nonuniform heating increases the length of the thermal entrance region. The noncircular geometry of the duct cross section may also be a contributing factor.

Fully Developed Nusselt Numbers. It is relevant to compare the fully developed Nusselt numbers to literature information and to seek the best possible correlation. From the literature, we take the venerable Dittus-Boelter correlation and the newer Petukhov-Popov correlation [1], respectively

$$Nu = 0.023Re^{0.8}Pr^{0.4} \quad (7)$$

and

$$\text{Nu} = (f/8)\text{RePr}/(1.07 + 12.7(\text{Pr}^{2/3} - 1)(f/8)^{1/2}) \quad (8)$$

where

$$f = (1.82 \log_{10}\text{Re} - 1.64)^{-2} \quad (9)$$

Both of these correlations were developed for circular tubes and are specified to be applicable for Re > 10,000.

Equations (7–9) have been evaluated using the hydraulic-diameter Reynolds numbers and are compared with the present data in Fig. 8. For Re > 10,000, the Dittus-Boelter equation overpredicts the data by about 30 percent, while the Petukhov-Popov equation is about 15 percent above the data.[3] Although this comparison adds further confirmation of the superiority of the Petukhov-Popov correlation relative to that of Dittus-Boelter, it also demonstrates that the hydraulic diameter does not provide an adequate rationalization of the noncircular geometry.

In considering the causes of less-than-successful performance of the literature correlations, specifically Petukhov-Popov, note may be taken of Fig. 3 which indicates that the circular-tube friction factor results deviate from those of the equilateral triangular duct, even when the hydraulic diameter is employed. This suggests the use of the measured triangular-duct friction factors as input to the Petukhov-Popov equation (8), replacing the circular-tube friction factor equation (9). When this is done, a duct-specific Petukhov-Popov prediction is obtained, as shown in Fig. 9 along with the experimental data. For Re > 10,000, the duct-specific prediction agrees with the data in the 1–5 percent range. This level of agreement is actually better than that achieved when the Petukhov-Popov correlation is compared with circular tube data.

Although a fully certain recommendation cannot be made at this time, it appears reasonable, when employing the Petukhov-Popov correlation for a noncircular duct, to input the friction factors for that duct, provided that they are available.

As an alternative correlation of the present data, a power-law fit yields

$$\text{Nu} = 0.019\text{Re}^{0.781} \quad (10)$$

to an accuracy of about four percent.

The present data will now be compared with the results of the turbulent-flow finite-difference solutions of [2]. For these solutions, the thermal boundary condition was circumferentially uniform temperature (on all three walls) and axially uniform heat input. Numerical results are reported only for Re > 40,000. Comparison with the present data for the two highest Reynolds numbers yields agreement within four percent (the prediction being high). This excellent level of agreement lends support to the analytical model and its numerical implementation.

Natural Convection Effects. Out of concern for possible natural convection effects, supplementary data runs were made for each of the two lowest Reynolds numbers such that the Grashof number was varied by a factor of two, from 6×10^3 to 1.3×10^4. The Grashof number variation had no detectable effect on the Nusselt number [6], and it was thus concluded that natural convection effects were negligible.

Concluding Remarks

The experiments reported here were designed with unusual care and attention to detail in order to provide research results of such quality as to serve as a standard against which analysis can be compared. Special techniques were employed to minimize extraneous heat conduction. Numerical finite-different solutions played an important role in both the design of the apparatus and in the data reduction.

The friction factor data underscored the fact that the hydraulic diameter is not completely successful in bringing circular tube correlations into agreement with noncircular duct results. The data did, however, support the predictions of a general noncircular duct correlation [8] as well as those from numerical solutions of a modeled turbulent flow [2].

Nusselt numbers were determined both in the thermal entrance region and in the fully developed region of the duct. The length of the entrance region increased markedly with Reynolds number. Entrance lengths, based on a five percent approach to fully developed conditions, ranged from 18 to 40 hydraulic diameters over the Reynolds number range from 6700 to 57,000. These lengths are greater than those for conventional duct flows (for air) and are believed to reflect the unsymmetric heating.

The experimentally determined fully developed Nusselt numbers were compared with both the Dittus-Boelter and Petukhov-Popov circular tube correlations (applicable for Re > 10,000), with the hydraulic diameter replacing the tube diameter. Although the latter correlation yielded better agreement with the data than did the former, it was still about 15 percent high. When the measured friction factors were used as input to the Petukhov-Popov equation, agreement between prediction and experiment to better than five percent was attained. This finding suggests that for a noncircular duct, the Petukhov-Popov equation be evaluated with the friction factor specific to that duct. The present data also support the Nusselt number predictions of [2] obtained via finite-difference solutions of a modeled turbulent flow.

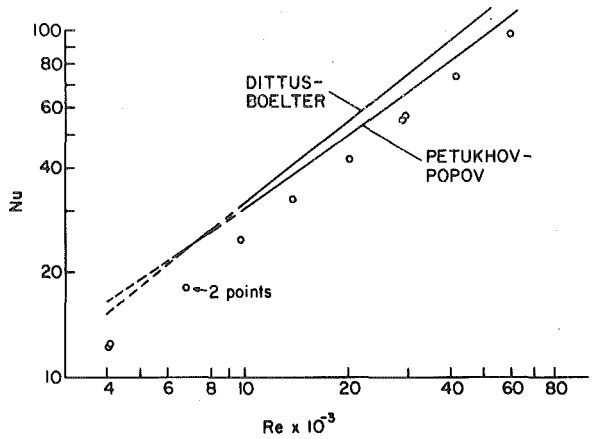

Fig. 8 Fully developed Nusselt numbers and comparisons with literature correlations

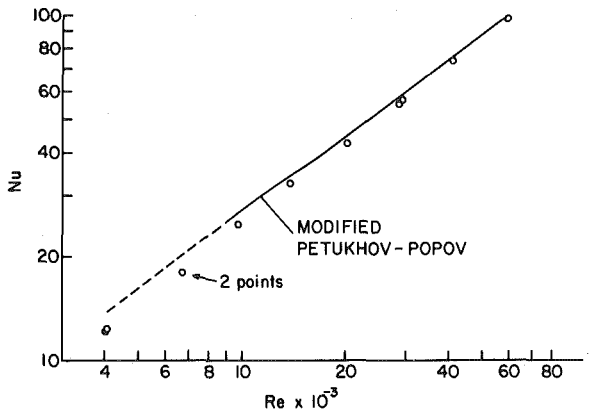

Fig. 9 Comparison of measured fully developed Nusselt numbers with the Petukhov-Popov correlation evaluated with the measured friction factors as input

Acknowledgment

This research was performed under the auspices of the Office of Naval Research (contract No. N00014-79-C-0621). Scholarship support was accorded to C.A.C. Altemani by CNPq and UNICAMP, both Brazilian Institutions.

[3] The Sleicher-Rouse correlation [10] is within about one-half percent of Petukhov-Popov.

References

1 Petukhov, B. S., "Heat Transfer and Friction in Turbulent Pipe Flow with Variable Physical Properties," *Advances in Heat Transfer,* Vol. 6, Academic Press, 1972, pp. 503–564.

2 Aly, A. M. M., Trupp, A. C., and Gerrard, A. D., "Measurements and Prediction of Fully Developed Turbulent Flow in an Equilateral Triangular Duct," *Journal of Fluid Mechanics,* Vol. 85, 1978, pp. 139–149.

3 Lowdermilk, W. H., Weiland, W. F., and Livingood, J. N. B., "Measurement of Heat Transfer and Friction Coefficients for Flow of Air in Non-Circular Ducts at High Surface Temperatures," NACA RM E53J07, 1954.

4 Eckert, E. R. G. and Irvine, T. F., "Pressure Drop and Heat Transfer in a Duct with Triangular Cross Section," ASME JOURNAL OF HEAT TRANSFER, Vol. 82, 1960, pp. 125–138.

5 Campbell, D. A., and Perkins, H. C., "Variable Property Turbulent Heat and Mass Transfer for Air in a Vertical Rounded Corner Triangular Duct," *International Journal of Heat and Mass Transfer,* Vol. 11, 1968, pp. 1003–1012.

6 Altemani, C. A. C., "Turbulent Heat Transfer and Fluid Flow Characteristics for Air Flow in an an Unsymmetrically Heated Triangular Duct," Ph.D. Thesis, Department of Mechanical Engineering, University of Minnesota, Minneapolis, Minn., 1980.

7 Sparrow, E. M., and Altemani, C. A. C., "On Attaining Isothermal Convectively Cooled Surfaces with Rear-Side, Discrete Groove-Embedded Heaters," *Numerical Heat Transfer,* Vol. 2, 1979, pp. 129–136.

8 Malak, J., Hejna, J., and Schmid, J., "Pressure Losses and Heat Transfer in Non-Circular Channels with Hydraulically Smooth Walls," *International Journal of Heat and Mass Transfer,* Vol. 18, 1975, pp. 139–149.

9 Knowles, G. R. and Sparrow, E. M., "Local and Average Heat Transfer Characteristics for Turbulent Airflow in an Asymmetrically Heated Tube," ASME JOURNAL OF HEAT TRANSFER, Vol. 101, 1979, pp. 635–641.

10 Sleicher, C. A., and Rouse, M. W., "A Convenient Correlation for Heat Transfer to Constant and Variable Property Fluids in Turbulent Pipe Flow," *International Journal of Heat and Mass Transfer,* Vol. 18, 1975, pp. 677–683.